Available online at www.sciencedirect.com
SCIENCE DIRECT®
Thin Solid Films 445 (2003) 186–192
thin solid films
www.elsevier.com/locate/tsf

# Key structural and defect chemical aspects of Cd–In–Sn–O transparent conducting oxides

T.O. Mason[a,*], D.R. Kammler[a,1], B.J. Ingram[a], G.B. Gonzalez[a], D.L. Young[b], T.J. Coutts[b]

[a]*Northwestern University, Department of Materials Science and Engineering and Materials Research Center, 2220 Campus Drive, Evanston, IL 60208, USA*
[b]*National Renewable Energy Laboratory, Golden, CO 80401, USA*

**Abstract**

The equilibrium phase diagram (1175 °C in air), solubility ranges and room temperature physical properties (electrical, optical) were established for the various n-type transparent conductors in the $CdO–In_2O_3–SnO_2$ system. Extended solubility ranges were found to exist at constant Cd/Sn ratio for the bixbyite, spinel and orthorhombic perovskite phases. This is attributed to the isovalent and nearly size-matched nature of the co-substitution. Still larger solubility ranges were found for metastably-processed thin films. Co-doped bixyite and spinel phases were found to be inherently off-stoichiometric with respect to cation composition, leading to self-doped n-type character, in bulk and films. A correlation was found between optimized conductivity in the various phases and the density of octahedral Cd, In and/or Sn species in their crystal structures.


*Keywords:* Cd–In–Sn–O system; Transparent conducting oxide (TCO); Bixbyite; Spinel; Perovskite

## 1. Introduction

Oxides of zinc, cadmium, indium and tin are well known for their unique combination of visible transparency and excellent n-type electrical conductivity. These materials are referred to as 'transparent conducting oxides' or TCOs, and find applications as low-emissivity coatings for windows and as transparent conductors in solar cells, flat panel displays, organic light-emitting diodes, etc. Since the pioneering works of Shannon et al. [1] on bulk TCOs and Frank and Köstlin [2] and Hamberg and Granqvist [3] on thin film TCOs, there have been ongoing efforts to understand the fundamental structural and chemical factors underlying their transparent conductivity. The present work explores composition–structure–property relationships in the $CdO–In_2O_3–SnO_2$ system.

The $CdO–In_2O_3–SnO_2$ phase diagram, shown in Fig. 1, is of interest for scientific and technological reasons. With the exception of ZnO and ZnO-based TCOs, the best reported and commercially viable TCOs come from this system. For example, each of the end-members—cadmium oxide, indium oxide and tin oxide—are TCOs in their own right. Suitably donor-doped $SnO_2$ and $In_2O_3$ (e.g. indium-tin oxide or 'ITO') are the most commercially utilized TCOs. The existence of alternative crystal structures (binary compounds) and ternary solid solution phases in the diagram, each of which are TCOs, make this a rich system for investigation. All share the common feature of continuous networks of cation octahedra, as pointed out by Shannon et al. [1] Furthermore, as we will show, they have common defect chemical processes, which are responsible for carrier generation and the resulting TCO properties.

Our methodology has been to combine bulk synthesis and thin film deposition, with characterization of structural, chemical and physical properties. The bulk phase diagram is an important baseline, establishing thermodynamic stability and solubility ranges for the various phases. Thin films, however, allow for extended (metastable) solubility ranges and more fundamental composition–structure–property studies.

*Corresponding author. Tel.: +1-847-491-3198; fax: +1-847-491-7820.
*E-mail address:* t-mason@northwestern.edu (T.O. Mason).
[1] Current address: Sandia National Laboratories, Albuquerque, NM 87185, USA.

0040-6090/03/$ - see front matter © 2003 Elsevier Science B.V. All rights reserved.
doi:10.1016/j.tsf.2003.08.012

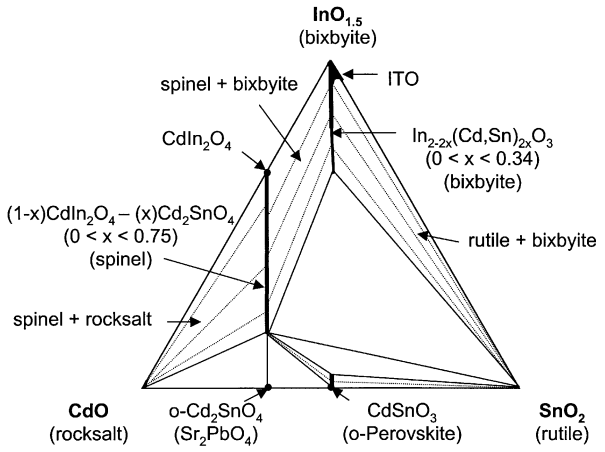


Fig. 1. Subsolidus phase relations in the $CdO–InO_{1.5}–SnO_2$ system at 1175 °C (after [4]).

## 2. Experimental

The subsolidus phase relations in the $CdO–In_2O_3–SnO_2$ system were studied by standard solid state reaction method at 1175 °C in air [4]. Pressed compacts of high purity component oxides (>99.99%) were reacted in alumina crucibles inside sacrificial powder beds of identical composition, with tightly fitting covers to limit volatilization. Repeated firing and grinding steps were used to achieve phase-purity, as determined by X-ray diffraction (XRD). Peak positions, corrected for off-axis displacement and zero-shift errors, were measured vs. a silicon internal standard. Solubility limits were established by Vegard's Law. In certain cases, intentionally biphasic assemblages were prepared to saturate a majority TCO phase with a small amount of second phase, allowing for electrical properties of the terminal composition to be measured. To enhance carrier content, bulk specimens were annealed at 400 °C for 4 h in forming gas (4% $H_2$/balance $N_2$).

Room temperature DC electrical conductivity was measured on sintered pellets (50–60% dense) using a standard four-probe device (Cascade Microtech, Beaverton, OR), with corrections for pellet geometry and also for porosity using the Bruggeman symmetric medium equation for continuous interconnected porosity [5]. Room temperature thermopower measurements were made by sandwiching pellets between a heat source and cold sink with gold foil electrodes (and welded thermocouples). Thermovoltages and temperature differences were monitored during the decay of a short heat pulse, from which the Seebeck coefficient was obtained. Diffuse reflectance measurements were made by double-beam spectrophotometer with an integrating sphere (Cary 1E with Cary 1/3 attachment, Varian, Walnut Creek, CA) relative to a PTFE powder compact standard. Diffuse reflectance vs. wavelength is analogous to transmission in films, and provides an estimate of the absorption edge and optical band gap of bulk specimens.

Thin films were deposited by r.f. magnetron sputtering between 580 and 660 °C under high purity oxygen at pressures between 15 and 70 mTorr. Oxide targets were hot-pressed by Cerac Inc. (Milwaukee, WI) from phase-pure powders of identical composition. Substrates were Corning 7059 glass (Corning, NY). Film thicknesses, measured by profilometer (Dektak 3, Veeco, Plainview, NJ), were varied between 0.1 and 1 μm. As-deposited films were subjected to a reduction anneal in argon gas or in the presence of a CdS, as described elsewhere [6]. Optical transmittance was measured on a Cary 5G UV/visable/IR spectrophotometer (Varian, Walnut Creek, CA), with optical gaps estimated by standard intercept method (plots of $(h\nu\alpha)^2$ vs. $h\nu$). Conductivity, carrier density and mobility were measured on a Bio-Rad Hall System (HL 5500, Bio-Rad, Cambridge, MA).

## 3. Results and discussion

### 3.1. Equilibrium phases and solubilities

Fig. 1 shows the subsolidus phase relationships at 1175 °C in air for the $CdO–In_2O_3–SnO_2$ system. In addition to the end-members, there are three binary compounds—$CdIn_2O_4$ (spinel structure), $Cd_2SnO_4$ (orthorhombic $Sr_2PbO_4$ structure) and $CdSnO_3$ (orthorhombic perovskite structure). Although there are no ternary compounds in the system, one of the unary compounds (bixbyite) and two of the binary compounds (spinel, *o*-perovskite) have solubility ranges extending at length into ternary phase space. Our prior work has shown that each of the 6 distinct phases/structures (rocksalt CdO, bixbyite $In_2O_3$, rutile $SnO_2$, strontium plumbate $Cd_2SnO_4$, spinel $CdIn_2O_4–Cd_2SnO_4$, orthorhombic perovskite $CdSnO_3$) plus the co-doped bixbyite solid solution is a good-to-excellent TCO [4]. The only exception to this is $SnO_2$, for which there is no suitable donor species in the Cd–In–Sn–O system. ($SnO_2$ is routinely rendered conducting by fluorine or antimony doping.) The $CdO–In_2O_3–SnO_2$ system is, therefore, rich in known and potential TCO materials.

The solid solution ranges in Fig. 1 are essentially vertical lines, which reflect the isovalent nature of the co-substitution process in each case. For example, co-substitution of either $In_2O_3$ or $CdIn_2O_4$ by CdO and $SnO_2$ in equal amounts can be represented as [7]:

$$CdO + SnO_2 + 2In_{In}^{x} \rightarrow Cd'_{In} + Sn_{In}^{\bullet} + In_2O_3 \quad (1)$$

such that there is a balance between acceptors and donors, i.e. $[Cd'_{In}] = [Sn_{In}^{\bullet}]$; two trivalent cations are being replaced by one divalent cation and one tetravalent cation. The reverse takes place in the orthorhombic perovskite phase, with two trivalent cations replacing

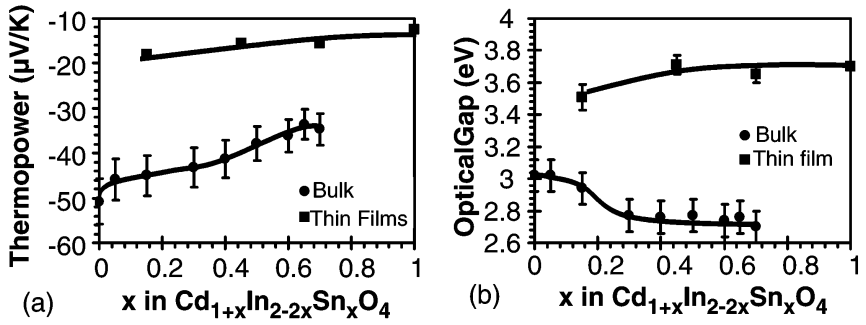


Fig. 2. (a) Thermopower vs. composition for bulk spinel specimens reduced in forming gas (4% $H_2$ and 96% $N_2$) and thin film spinel specimens annealed in Ar/CdS (after [13]). (b) Optical gaps vs. composition for bulk spinel specimens reduced in forming gas (4% $H_2$ and 96% $N_2$) and thin film spinel specimens annealed in Ar/CdS (after [13]).

one divalent cation and one tetravalent cation [7]:

$$In_2O_3 + Cd_{Cd}^{x} + Sn_{Sn}^{x} \rightarrow In_{Cd}^{\bullet} + In'_{Sn} + CdSnO_3 \qquad (2)$$

again preserving electroneutrality by self-compensation, i.e., a balance between donors and acceptors, $[In_{Cd}^{\bullet}] = [In'_{Sn}]$. It should also be pointed out that the average of the octahedral $Cd^{2+}$ and $Sn^{4+}$ radii (0.95 Å and 0.69 Å, respectively) is virtually identical to that of $In^{3+}$ (0.80 Å) [8].

The extended solubility ranges—4.5 cation percent in $CdSnO_3$, 34 cation percent in $In_2O_3$, and 75 cation percent in $CdIn_2O_4$—suggest the possibility for 'band structure engineering' of TCOs, not unlike what is done for compound semiconductors. Fig. 2 shows thermopower vs. composition (Fig. 2a) and optical gap vs. composition (Fig. 2b) for the spinel phase in the Cd–In–Sn–O system at room temperature. In spite of the forming gas treatment, the bulk specimens had much lower carrier contents than the corresponding CdS-treated films. In both cases, however, carrier content increased with the level of co-substitution, i.e. $x$ in $Cd_{1+x}In_{2-2x}Sn_xO_4$, which was substantiated by bulk conductivity measurements and Hall effect measurements on the films [8,9]. The noticeable drop in optical gap for the bulk specimens over the range $0 < x < 0.3$, in a direction contrary to the typical Burstein–Moss shift, suggests that there is a change in band structure or fundamental gap, with co-substitution. The wide ternary solubility ranges of the unary (bixbyite) and binary phases (spinel, *o*-perovskite) in the $CdO–In_2O_3–SnO_2$ system provide a means of tailoring the fundamental gap of these materials for optoelectronic applications. At the same time, less costly elements (Cd, Sn) are substituted for the more costly indium.

### 3.2. Metastable thin film solubilities

It is well known that the solubility ranges in thin films can be significantly greater than in bulk (equilibrium) specimens. Fig. 3 shows the Cd–In–Sn–O phase diagram modified to show reported single-phase composition ranges in thin films. It should be pointed out that these solubility ranges are metastable in nature, and highly dependent on the processing method. For example, Frank and Köstlin reported up to 22 cation percent Sn substitution for In in ITO films [2]. Polycrystalline films of In-doped CdO grown on glass substrates by metal–organic chemical vapor deposition (MOCVD) were shown to be phase-pure out to $x = 0.11$ in $Cd_{1-x}In_xO$ [10,11]. Epitaxial films of Sn-doped CdO grown by pulsed laser deposition (PLD) on (111) MgO substrates were similarly phase-pure out to $x = 0.11$ in $Cd_{1-x}Sn_xO$ [12]. Whereas the spinel solid solution is limited to the range $0 \leq x \leq 0.75$ in bulk $(1-x)CdIn_2O_4–xCd_2SnO_4$, thin films can be grown over the entire range, including pure $Cd_2SnO_4$ [6,13].

There are many factors, which could account for the extended solubility ranges in thin films. Substrate-induced strain and/or grain size effects can be discount-

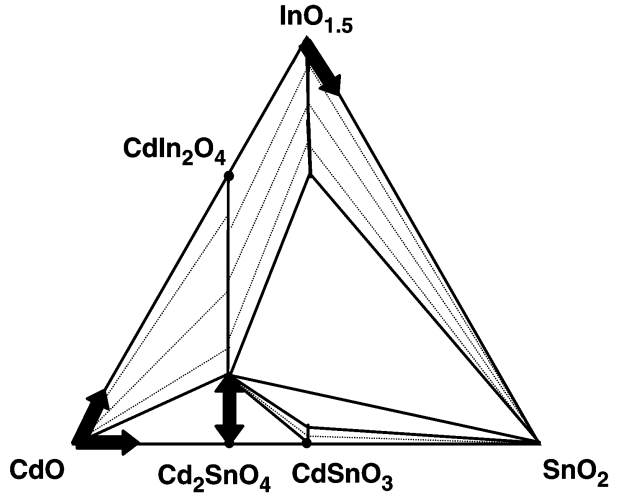


Fig. 3. The 1175 °C (air) subsolidus phase diagram of the CdO–$In_2O_3$–$SnO_2$ system, showing metastable extensions of solubility in the thin films (see text).

ed, due to the thickness of the films and the similarity in solubility limits between polycrystalline and epitaxial films. In the case of the vertical solid solutions in Figs. 1 and 3, we have already alluded to the isovalent and roughly size-matched nature of the co-substitution. Based upon structure field maps (A cation radius vs. B cation radius) for compounds with $A_2BO_4$ stoichiometry, $Cd_2SnO_4$ is on the borderline between the spinel and strontium plumbate structures [14]. This implies that the thermodynamic stabilities of the two phases are quite similar, which may help explain why the non-equilibrium spinel form of $Cd_2SnO_4$ so readily forms by metastable thin film processing.

Point defect association/clustering may also help facilitate the extended doping levels achievable in thin films. For example, we confirmed the presence of oxygen interstitials in ITO by Rietveld analysis of combined X-ray and neutron diffraction data from quenched bulk and nanocrystalline specimens [15]. The ratio of Sn-dopant species to oxygen interstitials was approximately 2:1 in oxidized specimens. The proposed doping mechanism is [2,15]:

$$2SnO_2 \rightarrow (2Sn_{In}^{\bullet}O''_i)^x + 3O_O^x \quad (3)$$

Under reducing conditions, the neutral associates ionize as follows:

$$(2Sn_{In}^{\bullet}O''_i)^x \leftrightarrow 1/2O_2(g) + 2Sn_{In}^{\bullet} + 2e' \quad (4)$$

However, the resulting carrier content is always significantly less than the overall Sn-doping level. Frank and Köstlin [2], who originally proposed this model, suggested that higher order complexation of the 2:1 Sn donor–oxygen interstitial associate leads to the formation of 'non-reducible' clusters. One indication that such clusters exist is the unusual variation of carrier content with doping level in thin films. Following an initial linear doping regime (where $n \sim [Sn_{In}^{\bullet}]$), the carrier content plateaus and eventually decreases with increasing Sn-content [2]. Similar behavior is observed in Sn- and In-doped CdO thin films [16]. Carrier content initially increases (up to 1% Sn or 3% In), plateaus and finally decreases at the highest doping level (approx. 11%). There has been no explanation to date for this behavior, but one potential defect mechanism is:

$$SnO_2 \rightarrow (Sn_{Cd}^{\bullet\bullet}V''_{Cd})^x + 2O_O^x \quad (5)$$

such that neutral associates are favored over electrons. Cation vacancies should be energetically favored over oxygen interstitials (as in Eq. (3)), given the absence of anion interstitices in the rocksalt structure of CdO, however, this hypothesis has yet to be confirmed.

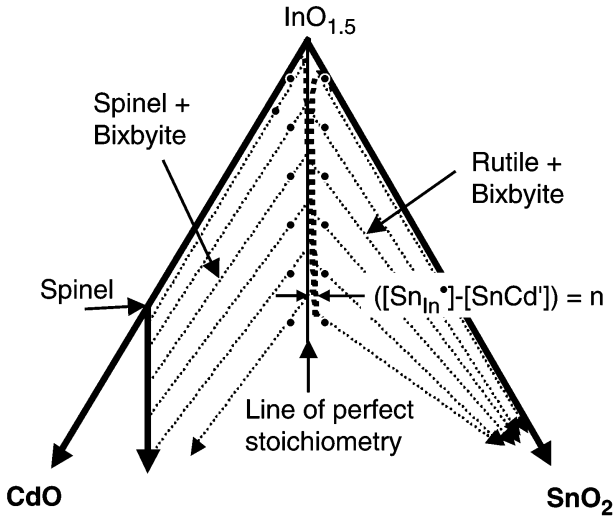


Fig. 4. Enlarged portion of the CdO–$In_2O_3$–$SnO_2$ diagram showing the bixbyite phase field (after [5]).

### 3.3. Self-doped ternary phases

The essentially isovalent co-substitution processes of Eqs. (1) and (2) do not result in carrier formation; there is a balance of donors and acceptors in each case. Nevertheless, all the ternary solid solutions in Fig. 1 prove to be n-type conductors. To understand their doping mechanism(s), intentionally biphasic assemblages were prepared, in which the TCO in question was the majority (approx. 95%) phase. In each case the second phase served to saturate the TCO majority phase at its solubility limit to either side of the vertical line in the phase diagram. For example, two series of compositions were prepared to either side of the bixbyite line of Fig. 1, as shown in the enlarged In-corner of the diagram in Fig. 4. Room temperature conductivities were measured and the ratio of Sn-rich vs. Cd-rich conductivities is plotted in Fig. 5a. Excess Sn-doping has a significant impact on the electrical conductivity (and carrier content) of undoped $In_2O_3$ (ITO) and lightly co-substituted specimens, but its influence decreases with increasing co-substitution. The 35% co-substituted material has the same conductivity under Sn-saturated vs. Cd-saturated conditions.

We have also taken nominally stoichiometric specimens (on the vertical line of Fig. 1) and subjected them to a reduction anneal at 400 °C for 6 h in forming gas (4% $H_2$/balance $N_2$). Fig. 5b plots the ratio of reduced conductivity to as-prepared conductivity. Undoped or lightly co-doped $In_2O_3$ specimens exhibit large conductivity increases upon reduction. Higher levels of co-doping, however, lead to specimens, which are relatively insensitive to hydrogen-reduction. This was substantiated by room temperature thermopower measurements

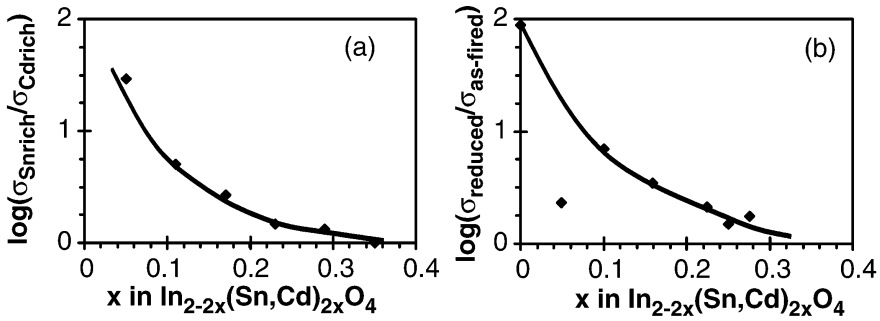


Fig. 5. (a) Plot of the ratio of room temperature conductivities for Sn-saturated vs. Cd-saturated bixbyite specimens (after [5]). (b) Plot of the ratio of room temperature conductivities for forming gas-reduced vs. as-fired specimens (after [5]).

[5]; carrier content changes very little during reduction for highly co-doped materials.

We have interpreted these behaviors as being indicative of the phase field location and width as indicated by the dotted curves in Fig. 4. For undoped and lightly co-doped $In_2O_3$, there is significant field width to the Sn-rich side of the vertical line of perfect stoichiometry. The width narrows, however, with higher levels of co-substitution, and the location shifts in the direction of excess Sn. This results in an imbalance of donor vs. acceptor species, i.e. $n = \{[Sn_{In}^{\bullet}] - [Cd'_{In}]\} > 0$. Fig. 6 shows a schematic diagram of free energy vs. doping. The solid curve shows the situation for lightly co-doped $In_2O_3$. There is little or no excess Cd-solubility (acceptor-doping); to date there is no indication of p-type behavior in any of the phases in the $CdO-In_2O_3-SnO_2$ system. There is, however, considerable excess Sn-solubility (donor-doping), as in ITO. With increased co-doping, however, the stability range narrows (as shown in Fig. 4) and shifts away from the fully compensated (perfect stoichiometry) situation in favor of excess Sn (donor-doping). (It must be noted that there is a small detectable solubility of CdO in $In_2O_3$. As pointed out previously [7], this appears to produce ionic compensation (by oxygen vacancies) instead of holes; the resulting material is highly resistive and remains n-type).

A similar cation off-stoichiometry has been found for the spinel solid solution [8]. Electron probe microanalysis of the thin films prepared in this study showed final compositions that increasingly shifted from nominal (or perfect) stoichiometry in the Sn-rich in a fashion analogous to the behavior in Fig. 4. As with the bixbyite specimens, bulk Cd-saturated specimens were excellent n-type conductors, only slightly less conductive than Sn-saturated specimens. It follows that the spinel phase exhibits a similar tendency toward excess Sn (donor) excess, as per the dashed curve in Fig. 6. The inherent cation off-stoichiometry results in an excess of donors over acceptors, i.e. $n = \{[Sn_{In}^{\bullet}] - [Cd'_{In}]\}$.

It follows that such co-substituted materials are 'self-doped' TCOs. In the case of co-doped bixbyite, the terminal solid solution is only a factor of three less conductive than comparably prepared bulk ITO. It is relatively insensitive to the state of oxidation/reduction and, therefore, does not require a reduction anneal to improve its conductivity. Conversely, such materials are robust TCOs, being relatively immune to redox reactions during device processing, which might otherwise result in inadvertent under- or over-doping by carriers. The spinel phase is particularly noteworthy in this regard. $CdIn_2O_4-Cd_2SnO_4$ materials were forgiving with respect to overall composition and the processing conditions employed, including deviations from nominal cation stoichiometry and/or variable redox conditions, and proved to be excellent TCOs [4].

### 3.4. Chemical and structural aspects

In their pioneering work on TCOs, Shannon et al. concluded that 'continuous edge sharing of $Cd^{2+}$, $In^{3+}$

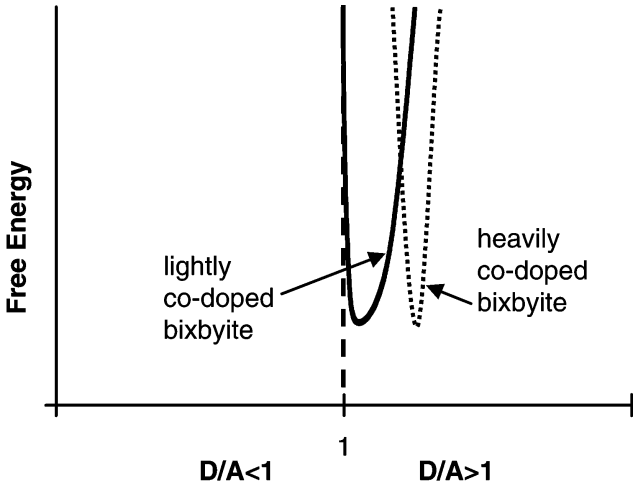


Fig. 6. Schematic of free energy vs. doping in co-doped bixbyite. (D/A = donor-to-acceptor ratio).

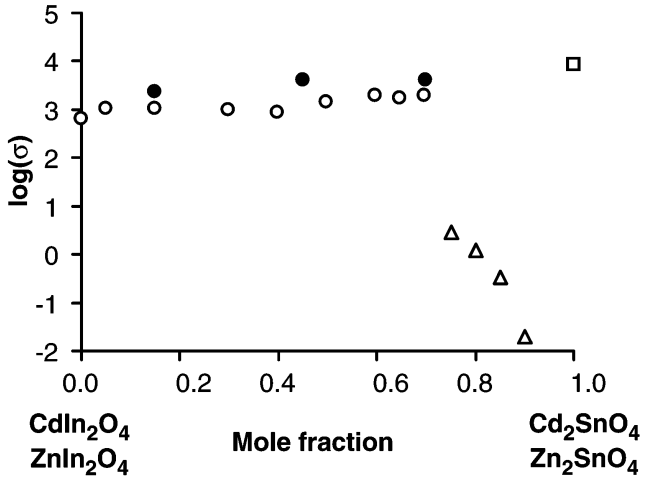


Fig. 7. Comparison of room temperature conductivities for $(1-x)CdIn_2O_4$–$xCd_2SnO_4$ (○=bulk, ●=thin film, this work; $x=1$, □, [6]) and bulk $(1-x)ZnIn_2O_4$–$xZn_2SnO_4$ (△, [17]).

and $Sn^{4+}$ octahedra is a necessary criterion for the formation of a transparent conductor' [1]. Kawazoe and Ueda [17] similarly described the potential importance of 'rutile chains' or 'pathways' of edge-shared octahedral along the ⟨110⟩ direction in the spinel structure. Our work is consistent with these statements, with the amendment that corner-shared octahedra, e.g. in orthorhombic $CdSnO_3$, also result in transparent conductivity.

Fig. 7 plots conductivity vs. composition for bulk and thin film specimens of the $(1-x)CdIn_2O_4$–$xCd_2SnO_4$ spinel phase, including pure cadmium stannate [6]. For comparison purposes, the conductivity vs. composition behavior of the corresponding $(1-x)ZnIn_2O_4$–$xZn_2SnO_4$ spinel solid solution [18] is also plotted (bulk specimens). Although solid solubility is limited to $x>0.75$ in the latter case, the comparison is instructive. Like $Cd_2SnO_4$, $Zn_2SnO_4$ is an inverse spinel, with $Sn^{4+}$ in octahedral sites exclusively, and the divalent species divided between tetrahedral and octahedral sites [13,18,19]. What these data show is that the combination of Zn and Sn on octahedral sites is not as effective as Cd and Sn in yielding good TCO behavior. This may be due to in part to $Zn_2SnO_4$ (and solid solutions) being more nearly cation-stoichiometric [19], such that the electron population, $n=\left\{[Sn_{In}^{\bullet}]-[Cd'_{In}]\right\}$, remains small. Young et al. [19] detected the presence of two distinct octahedral environments for $Sn^{4+}$ in $Zn_2SnO_4$ by Mössbauer Spectroscopy, and speculated that this distortion was responsible for a relatively low electron mobility. It is also noteworthy that the tetrahedral Zn species do not appear to contribute significantly to the overall conductivity. This may be due to the ~20% larger Zn–Zn distances in $Zn_2SnO_4$ vs. that in ZnO.

In Fig. 8 we have plotted the 'best value' literature conductivities to date for the various TCO phases in the $CdO$–$In_2O_3$–$SnO_2$ system vs. the density (per $cm^3$) of octahedrally coordinated cations ($Cd^{2+}$, $In^{3+}$ and/or $Sn^{4+}$). No value is shown for $SnO_2$, for which there is no suitable donor in the Cd–In–Sn–O system (apart from oxygen vacancies). The value for the distorted orthorhombic perovskite ($CdSnO_3$) is taken from two sources, one bulk [2] and one thin film [20]. The value for orthorhombic $Cd_2SnO_4$ is for a bulk specimen [4]. The values for $Cd_2SnO_4$ [6], Sn-doped $In_2O_3$ [21] and In-doped CdO [22] are for thin film materials. (A still higher conductivity, ~40 000 S/cm, was reported for epitaxial Sn-doped CdO [12], however, the band gap was less than 3.0 eV in this material). Electron mobilities were only available for the films, but these were quite comparable in value (40–70 $cm^2/Vs$). The resulting plot is admittedly simplistic, but tends to support the contention of Shannon et al. [2], that the best TCO materials are those which concentrate Cd, In and/or Sn in a continuous network of octahedral sites. The best and simplest such structure is rocksalt (CdO), followed closely by bixbyite ($In_2O_3$). The other structures (spinel, strontium plumbate, *o*-perovskite) have substantial fractions of cations in other coordinations, thereby diluting the overall octahedral network.

## 4. Conclusions

The $CdO$–$In_2O_3$–$SnO_2$ system is rich in transparent conductors. No less than six distinct crystal structures—rocksalt (CdO), bixbyite ($In_2O_3$), rutile ($SnO_2$), orthorhombic perovskite ($CdSnO_3$), orthorhombic strontium plumbate ($Cd_2SnO_4$) and spinel ($CdIn_2O_4$, $Cd_2SnO_4$)—exist in the system, each of which is a good-to-excellent TCO. Isovalent and largely size-matched cation substitutions result in extensive solid solution ranges for the bixbyite, spinel and *o*-perovkite materials, which occur

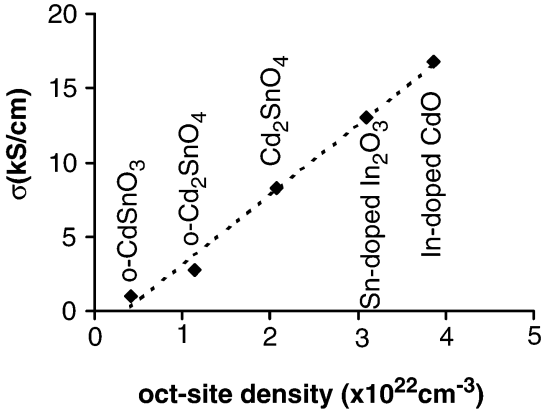


Fig. 8. 'Best value' reported conductivities for various TCO phases in the $CdO$–$In_2O_3$–$SnO_2$ diagrams (see text).

along lines of constant Cd/Sn ratio. This is due to the substitution of divalent Cd and tetravalent Sn for two trivalent In species, or vice versa. Such extended solubilities offer the prospect of 'band structure engineering' through variation of overall chemical composition. Metastable thin film processing in the $CdO-In_2O_3-SnO_2$ system yields still larger solubility ranges than for bulk materials. Defect complex formation may be one of several factors contributing to the enhanced solubilities in thin films. Subtle shifts in overall cation stoichiometry with co-substitution in the bixbyite and spinel structures lead to inherently 'self-doped' n-type materials, which do not require reduction processing for the production of carriers. A linear relationship has been found between optimized values of conductivity and the overall density of octahedral sites in the various TCO phases, all of which have in common interconnected networks of edge- or corner-shared octahedra. The best known n-type TCOs, which are found in the $CdO-In_2O_3-SnO_2$ system, have the highest concentration of Cd, In and/or Sn in octahedral coordination.

## Acknowledgments

This work was supported in part by the MRSEC program of the National Science Foundation (grant no. DMR-0076097) through the Materials Research Center of Northwestern University and in part by the Department of Energy (grant no. DE-FG02-84ER45097) through the National Renewable Energy Laboratory (subcontract AAD-9-18668-05). D.R. Kammler acknowledges the support of an NSF graduate fellowship and B.J. Ingram acknowledges the support of a NDSEG fellowship.

## References

[1] R.D. Shannon, J.L. Gillson, R.J. Bouchard, J. Phys. Chem. Solids 38 (1977) 877.
[2] G. Frank, H. Köstlin, Appl. Phys. A 27 (1982) 197.
[3] I. Hamberg, C.G. Granqvist, J. Appl. Phys. 60 (1986) R123.
[4] D.R. Kammler, B.J. Harder, N.W. Hrabe, N.M. McDonald, G.B. Gonzalez, D.A. Penake, T.O. Mason, J. Am. Ceram. Soc. 85 (2002) 2345.
[5] D.R. Kammler, T.O. Mason, K.R. Poeppelmeier, J. Am. Ceram. Soc. 84 (2001) 1004.
[6] X. Wu, T.J. Coutts, W.P. Mulligan, J. Vac. Sci. Technol. A 15 (1997) 1057.
[7] T.O. Mason, G.B. Gonzalez, D.R. Kammler, N. Mansourian-Hadavi, B.J. Ingram, Thin Solid Films 411 (2002) 106.
[8] D.R. Kammler, T.O. Mason, D.L. Young, T.J. Coutts, J. Appl. Phys. 90 (2001) 3263.
[9] R.D. Shannon, Acta Crystallogr. A 32 (1976) 751.
[10] J.R. Babcock, A. Wang, A.W. Metz, N.L. Edleman, M.V. Metz, M.A. Lane, C.R. Kannewurf, T.J. Marks, Adv. Matls. CVD 7 (2001) 242.
[11] R. Asahi, A. Wang, J.R. Babcock, N.L. Edleman, A.W. Metz, M.A. Lane, V.P. Dravid, C.R. Kannewurf, A.J. Freeman, T.J. Marks, Thin Solid Films 411 (2002) 101.
[12] M. Yan, M. Lane, C.R. Kannewurt, R.P.H. Chang, Appl. Phys. Lett. 78 (2001) 2342.
[13] D.R. Kammler, T.O. Mason, D.L. Young, T.J. Coutts, D. Ko, K.R. Poeppelmeier, D.L. Williamson, J. Appl. Phys. 90 (2001) 5979.
[14] O. Muller, R. Roy, The Major Ternary Structural Families, 4, Springer-Verlag, New York, 1974, p. 487.
[15] G.B. Gonzalez, J.B. Cohen, J.-H. Hwang, T.O. Mason, J. Appl. Phys. 89 (2001) 2550.
[16] R. Asahi, J.R. Babcock, N.L. Edleman, D.R. Kammler, D. Ko, M.A. Lane, A.W. Metz, A. Wang, M. Yan, R.P.H. Chang, V. Dravid, A.J. Freeman, C.R. Kannewurf, T.J. Marks, T.O. Mason, K.R. Poeppelmeier. Electrochemical Society Proceedings, Electrochemical Society, Pennington, NJ, 2001–10 (2001), p. 333.
[17] H. Kawazoe, K. Ueda, J. Am. Ceram. Soc. 82 (1999) 3330.
[18] G.P. Palmer, K.R. Poeppelmeier, T.O. Mason, J. Solid State Chem. 134 (1997) 192.
[19] D.L. Young, D.L. Williamson, T.J. Coutts, J. Appl. Phys. 91 (2002) 1464.
[20] G. Haacke, Appl. Phys. Lett. 28 (1976) 622.
[21] H. Ohta, M. Orita, M. Hirano, H. Hosono, J. Appl. Phys. 91 (2002) 3547.
[22] A. Wang, M. Lane, N.L. Edleman, A.W. Metz, M.A. Lane, R. Asahi, V.P. Dravid, C.R. Kannewurf, A.J. Freeman, T.J. Marks, Proc. Natl. Acad. Sci. 98 (2001) 7113.